Biochimica et Biophysica Acta 1853 (2015) 338–347

Contents lists available at ScienceDirect

Biochimica et Biophysica Acta

journal homepage: www.elsevier.com/locate/bbamcr

CD138-negative myeloma cells regulate mechanical properties of bone marrow stromal cells through SDF-1/CXCR4/AKT signaling pathway

Dan Wu [a,1], Xinyi Guo [b,1], Jing Su [a], Ruoying Chen [a], Dmitriy Berenzon [c], Martin Guthold [b], Keith Bonin [b], Weiling Zhao [a], Xiaobo Zhou [a,*]

[a] Department of Radiology, Wake Forest School of Medicine, Medical Center Boulevard, Winston-Salem, NC 27157, USA
[b] Department of Physics, Wake Forest University, Winston-Salem, NC 27109, USA
[c] Hematology & Oncology, Wake Forest School of Medicine, Medical Center Boulevard, Winston-Salem, NC 27157, USA

ARTICLE INFO

Article history:
Received 7 July 2014
Received in revised form 10 October 2014
Accepted 14 November 2014
Available online 21 November 2014

Keywords:
Multiple myeloma
Bone marrow stromal cell
Stiffness
CD138-negative
SDF-1/CXCR4
AKT

ABSTRACT

As the second most prevalent hematologic malignancy, multiple myeloma (MM) remains incurable and relapses due to intrinsic or acquired drug resistance. Therefore, new therapeutic strategies that target molecular mechanisms responsible for drug resistance are attractive. Interactions of tumor cells with their surrounding microenvironment impact tumor initiation, progression and metastasis, as well as patient prognosis. This cross-talk is bidirectional. Tumor cells can also attract or activate tumor-associated stromal cells by releasing cytokines to facilitate their growth, invasion and metastasis. The effect of myeloma cells on bone marrow stromal cells (BMSCs) has not been well studied. In our study, we found that higher stiffness of BMSCs was not a unique characteristic of BMSCs from MM patients (M-BMSCs). BMSCs from MGUS (monoclonal gammopathy of undetermined significance) patients were also stiffer than the BMSCs from healthy volunteers (N-BMSCs). The stiffness of M-BMSCs was enhanced when cocultured with myeloma cells. In contrast, no changes were seen in myeloma cell-primed MGUS- and N-BMSCs. Interestingly, our data indicated that $CD138^-$ myeloma cells, but not $CD138^+$ cells, regulated M-BMSC stiffness. SDF-1 was highly expressed in the $CD138^-$ myeloma subpopulation compared with that in $CD138^+$ cells. Inhibition of SDF-1 using AMD3100 or knocking-down CXCR4 in M-BMSCs blocked $CD138^-$ myeloma cells-induced increase in M-BMSC stiffness, suggesting a crucial role of SDF-1/CXCR4. AKT inhibition attenuated SDF-1-induced increases in M-BMSC stiffness. These findings demonstrate, for the first time, $CD138^-$ myeloma cell-directed cross-talk with BMSCs and reveal that $CD138^-$ myeloma cells regulate M-BMSC stiffness through SDF-1/CXCR4/AKT signaling.

1. Introduction

Multiple myeloma (MM) is a malignant neoplasm of plasma cells that accumulate in bone marrow. It accounts for 10% of all malignant hematological diseases [1]. According to the National Cancer Institute cancer statistics, 24,050 new cancer cases of MM will be diagnosed in the United States in 2014, and an estimated 11,090 deaths will occur [2]. In almost all of cases, MM is preceded by a premalignant disease called monoclonal gammopathy of undetermined significance (MGUS) [3,4]. MGUS affects 2% of the population above the age of 50 and progresses to overt MM at a rate of 1% per year [5]. Although discovery of novel therapeutics by targeting important disease-driving pathways has led to significant improvement in MM response and survival of patients, MM remains incurable due to relapse and drug resistance [6,7]. Therefore, understanding the mechanisms associated with MM pathogenesis is necessary for the development of novel targeting agents.

Growing evidence supports the hypothesis that cross-talk between myeloma cells and the bone marrow microenvironment plays an important role in myeloma cell growth and drug resistance [8]. The bone marrow niche includes cellular and noncellular compartments. The cellular compartments are composed of hematopoietic stem and progenitor cells, immune cells, erythrocytes, bone marrow stromal cells (BMSCs), endothelial cells, osteoclasts and osteoblasts. The noncellular compartments consist of various extracellular matrix (ECM) proteins, such as fibronectin, collagen, laminin and osteopontin, and the liquid milieu including cytokines, growth factors and chemokines. Interaction of myeloma cells with bone marrow microenvironments is crucial for MM pathogenesis. Myeloma cells adhere to BMSC or ECM not only for bone marrow homing, but also for activation of pleiotropic proliferative and anti-apoptotic cascades [9]. Adhesion of myeloma cells

Abbreviations: MM, multiple myeloma; BMSCs, bone marrow stromal cells; CD138, syndecan-1; SDF-1, stromal cell-derived factor 1; CXCR4, chemokine (C-X-C motif) receptor 4

* Corresponding author at: Department of Radiology, Wake Forest University School of Medicine, Medical Center Boulevard, Winston-Salem, NC 27157, USA. Tel.: +1 336 716 2011.
E-mail address: xizhou@wfubmc.edu (X. Zhou).

[1] These authors share first authorship.

http://dx.doi.org/10.1016/j.bbamcr.2014.11.019
0167-4889/

to BMSCs triggers NF-κB activation, initiates Notch signaling, and induces secretion of interleukin-6, vascular endothelial growth factor, insulin-like growth factor, and other factors [6,10,11], which have been associated with chemo-resistance of MM [12–14]. Our understanding of the contribution of the bone marrow microenvironment on cancer progression is still limited, that's why elucidating the role of the microenvironment is a major step in improving treatment of MM.

Cancer initiating cells are capable of continuous self-renewal and differentiation into mature cancer cells, and are predicted to be involved in drug resistance. $CD138^-$ myeloma cells have been considered as myeloma initiating cells. Matsui et al. first described CD138 negative ($CD138^-$) population with greater clonogenic potential than CD138 positive ($CD138^+$) myeloma cells [15,16]. $CD138^-$ clonotypic B cells are also found in the peripheral blood and bone marrow of patients with MM [16,17] and are associated with poor survival of MM patients [18]. Indeed, successful engraftment of $CD138^-$ subpopulation from MM patients, but not $CD138^+$, in NOD/SCID mice suggested that $CD138^-$ myeloma cells were the principal myeloma initiating cells [19]. $CD138^-$ myeloma cells express higher levels of aldehyde dehydrogenase [15,20] and are resistant to anti-MM drugs, such as lenalidomide [15,21].

Microenvironment stiffness plays a crucial role in cancer development and progression. In vitro studies indicate that the mechanical properties of the extracellular matrix have a great impact on cancer growth and differentiation [22–24]. The mechanical integrity of cells is regulated by a dynamic network of structural, cross-linking, and signaling molecules. A previous study reported that BMSCs collected from MM patients were stiffer than healthy BMSCs [25]. The interaction between BMSCs and myeloma stem cells has not been well studied. Feng et al. found that myeloma BMSCs stimulated growth and survival of myeloma initiating cells in vitro and in vivo, which was partially mediated via the SDF-1/CXCR4 signaling pathway [26]. Tumors have the ability to shape microenvironment by secreting growth factors, cytokines and chemokines to meet their needs for development. In this study, we determined the effect of myeloma cells on the stiffness of BMSCs and explored the molecular mechanisms underlying these mechanical changes. We found that BMSCs from MM (M-BMSC) and MGUS (MGUS-BMSC) patients were stiffer than normal BMSCs (N-BMSCs). The stiffness of M-BMSCs was enhanced when cocultured with myeloma cells. However, no changes were seen in the stiffness of myeloma cell-primed MGUS- and N-BMSCs. $CD138^-$ myeloma cells, but not $CD138^+$ cells, mediated the stiffness of M-BMSCs. SDF-1 was highly expressed in $CD138^-$ myeloma cells compared with that in $CD138^+$ cells. Inhibition of SDF-1 by a pharmacological inhibitor AMD3100 or knocking-down CXCR4 using siRNA abolished $CD138^-$ myeloma cells-induced increase in M-BMSC stiffness, suggesting a key role of SDF-1. Effects of SDF-1 on M-BMSC stiffness appear to be mediated by AKT.

2. Materials and methods

2.1. Isolation and expansion of BMSCs

Primary human BMSCs were derived from identified human whole bone marrow aspirates. Usage of these samples has been approved by the Institutional Review Board of The Methodist Hospital Research Institute (TMHRI) and Wake Forest University Health Science (WFUHS). BMSC isolation was conducted as previously described [26]. Bone marrow mononuclear cells were obtained by Ficoll density gradient (1.077 g/ml; Sigma, St. Louis, MO) and then plated into 35 cm^2 tissue culture flasks at a concentration of 10^6 cells/ml in Mesencult basal medium supplemented with MSC stimulatory supplements (Invitrogen, Vancouver, BC). After 24 h incubation at 37 °C in a 5% CO_2 humidified atmosphere, non-adherent cells were removed, and the adherent fraction was cultured with fresh medium. When reaching 60% confluence, cells were trypsinized (0.25% trypsin/EDTA, Gibco, Vancouver, BC) and replated into a 100 cm^2 tissue culture dish. The cells at fourth passages were cryopreserved in a liquid nitrogen tank and stored for subsequent experiments. The human marrow stromal cell lines HS5, derived from the marrow of a healthy volunteer were obtained from ATCC.

2.2. Atomic force microscope (AFM) assay

All cell stiffness measurements were performed using a combined atomic force microscope (AFM)/inverted optical microscope [27–29] at room temperature. The AFM (Topometrix Explorer, Veeco Instruments, Woodbury, NY) was situated above the sample and fit on a custom-designed stage of the inverted optical microscope (Axiovert 200, Zeiss, Thornwood, NY, USA). The optical microscope was equipped with a high sensitivity emCCD camera (EM-CCD C9100-02, Hamamatsu Photonics KK, Japan) and IPLab imaging software (Scanalytics, Fairfax, VA). The stage was designed so that the samples could be moved in the x- and y-directions independently when the AFM was sitting on the stage. We used tip-less AFM silicon probes (Applied Nano Structures Inc., USA) to which we attached 5.3 μm fluorescent melamine beads (Microspheres–Nanospheres, Cold Spring, NY). The AFM probes had nominal spring constants of $k = 0.1–0.6$ N/m, length $L = 225$ μm, and width, $w = 43$ μm. A more accurate spring constant was determined from the dimensions and the resonance frequency of the AFM probe, and our probes were calibrated against known gel standards, as described in more detail in [30]. The approaching and retraction speeds were 1 μm/s, with an indentation depth of 1.5 μm. Thus, the frequency was $(1\ \mu m/s) / (2 \times 1.5\ \mu m) = 0.33$ Hz. This frequency is a good, commonly used compromise between two opposing requirements for cell measurements. On the one hand it is slow enough to minimize viscous components, on the other hand is it fast enough to provide stable measurements on cells. Importantly, it is also slower than the typical speed with which cells move or change.

For each sample, 30–60 indentation measurements were collected over a period of 2 h. The number of cells for our measurement series is sufficiently large according to the standards of the AFM community [31]. All measurements were carried out in Mesencult basal medium. Data processing was done as described in previously published work [30].

2.3. $CD138^-$ myeloma cell isolation

NCI H929 human myeloma cells were obtained from ATCC and $CD138^-/CD138^+$ subpopulation was separated by a MACS separator, according to the manufacturer's instructions. CD138 microbeads, MACS Columns and MACS Separators were purchased from Miltenyi Biotec (Auburn, California). NCI H929 cells were suspended in 80 μl 0.5% MACS buffer and incubated with 20 μl of CD138 microbeads for 15 min at 4 °C. Place an MS column into the separator magnet. After wash, the cells were then resuspended in 500 μl MACS buffer and loaded onto MS MACS column. The magnetic labeled $CD138^+$ cells were bound to the column. The effluent containing non-labeled $CD138^-$ cells were collected in a 1.5 ml tube. The magnetic labeled $CD138^+$ cells were then released from magnetic field using 1 ml wash buffer.

2.4. Western blotting

Cells were lysed using RIPA buffer supplemented with protease and phosphatase inhibitor cocktail (Roche Applied Science, Indianapolis, IN) and stored in aliquots at −20 °C until use. Twenty micrograms of cell lysates was mixed with an equal volume of Laemmli sample buffer, denatured by boiling, and separated by SDS-PAGE. The separated proteins were then transferred to a nitrocellulose membrane (BioRad). The membranes were blocked using 5% non-fat dry milk for 1 h at room temperature and probed with anti-phospho-Akt (Ser473) rabbit mAb (Cell signaling, Beverly, MA), anti-phospho-RhoA (Ser188) rabbit mAb (Cell signaling), anti-phospho-Myosin light chain (Ser19) rabbit mAb (Cell signaling), anti-phospho-FAK (Tyr925) rabbit mAb (Cell

signaling), anti-Akt rabbit mAb (Cell signaling), and anti-phospho-CXCR4 (Ser339) rabbit mAb (Sigma-Aldrich, St. Louis, MO). After washing three times in TBST, the blots were incubated with IgG horseradish peroxidase conjugated anti-rabbit antibody (Cell signaling, Beverly, MA) at a final concentration of 1:5000 for 2 h at room temperature. Immunoblots were developed using the enhanced chemiluminescence (ECL) reagent (Cell signaling, Beverly, MA) and visualized using FluroChemQ processor (Proteinsimple, Santa Clara, CA).

2.5. RNA extraction and Real-time quantitative PCR

Total RNA was extracted using an RNeasy Micro kit (Qiagen, Santa Clarita, CA) according to the manufacturer's instructions. First-strand cDNA was synthesized using superscript III first-strand synthesis system (Invitrogen) according to the recommendations of the manufacturer. Briefly, 1 μg of total RNA, 0.5 μg of oligo dT and nuclear-free water were heated at 65 °C for 10 min and then chilled on ice for 5 min. Forty units of RNase inhibitor (Promega, Madison, WI), 3 μl of 100 mM DTT (GIBCO), 1 μl of 10 mg/ml bovine serum, 6 μl of 5× first-strand synthesis buffer, 2 μl of nuclear-free water, and 200 U superscript III reverse transcriptase were then added together and mixed well. The mixture was incubated at 50 °C for 50 min and at 85 °C for 10 min. Then the mixture was chilled on ice and incubated with RNase H at 37 °C for 20 min. Synthesized cDNA could be stored at −20 °C until use.

Quantitative real time PCR (qPCR) reactions were carried out on the 7500 Fast Real-time PCR system (Applied Biosystems, Foster City, CA). SDF-1 and β-actin SYBR based primers were obtained from RealTimePrimers (Elkins Park, PA). Briefly, 20 μl of reaction mixture was mixed with a 10 μl Power SYBR green PCR master mix (Invitrogen), 80 ng of cDNA, 300 nM of upstream and downstream primers and nuclear-free water. PCR reaction was conducted with 1 cycle at 95 °C for 10 min, 40 cycles at 95 °C for 15 s, 40 °C for 30 s and 60 °C for 1 min, followed by dissociation curve analysis distinguishing PCR

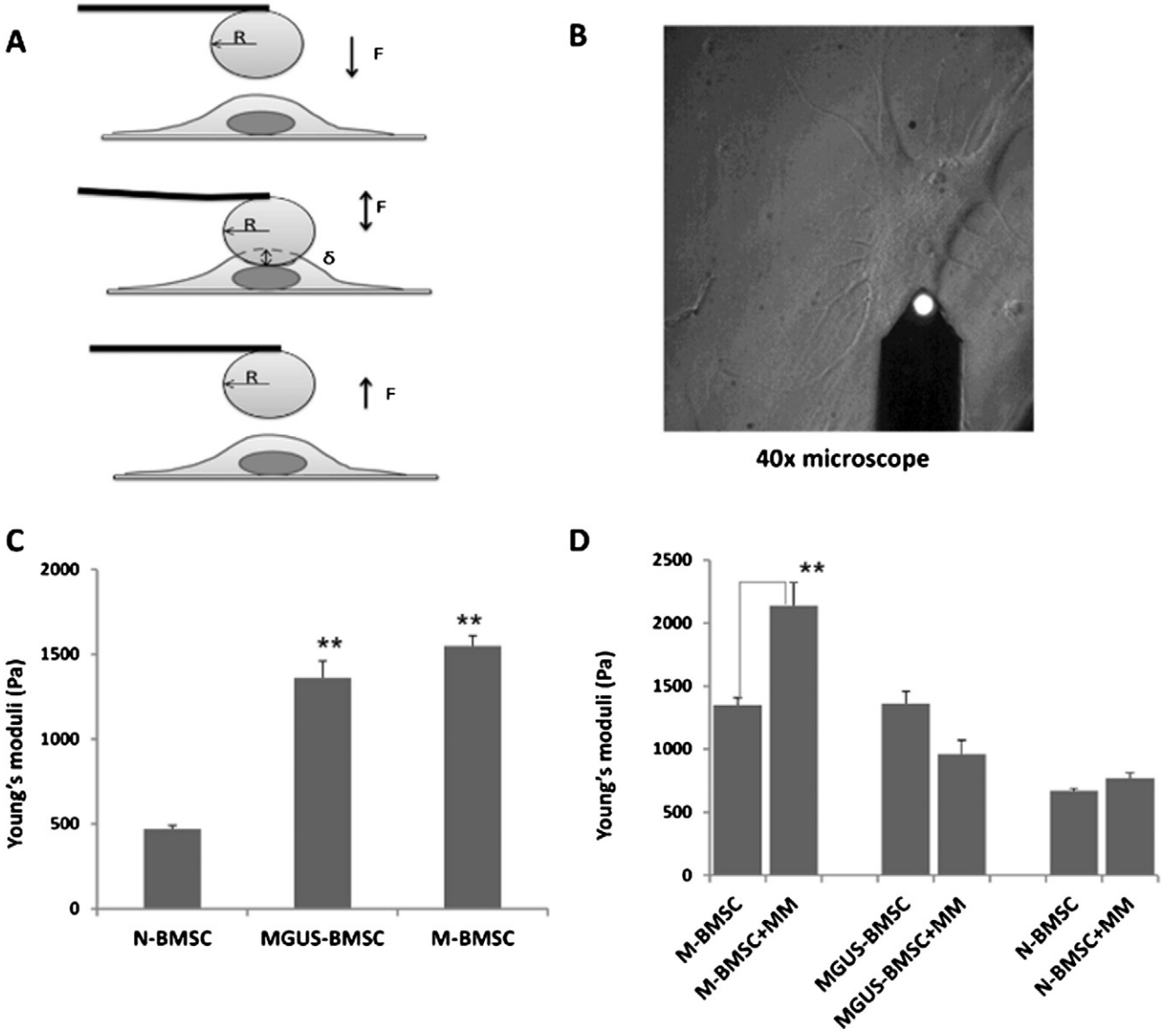

Fig. 1. Detect stiffness of BMSCs from MM, MGUS patients and normal volunteers using AFM (atomic force microscopy). A: schematic diagram showing detection of stiffness in a single cell using AFM. B: A representative fluorescence microscopy image (40× objective lens) showing an AFM cantilever (width 43 μm) with a fluorescent bead (5.3 μm diameter) approaching a cell. C: The stiffness of BMSCs collected from MM, MGUS and healthy volunteers was determined by AFM and expressed as Young's moduli. Data was collected from 60 cells of M-BMSCs, 43 MGUS-BMSCs and 47 N-BMSCs. D: BMSCs were co-cultured with NCI H929 myeloma cells for 24 h. The stiffness of BMSCs was measured after removing NCI H929 cells. Data was calculated from 52 cells of M-BMSCs, 30 MGUS-BMSCs and 57 N-BMSCs. All experiments were repeated 3 times. Mean ± SE; **$p < 0.01$.

products. The average ΔΔCT and standard deviation were determined from three independent experiments.

2.6. Coculture of BMSCs and myeloma cells

BMSCs at passage 3–6 were cultured in 35 mm dishes. When BMSCs reached 40%–60% confluence, NCI H929 cells were then added into the same culture dish and incubated for 24 h. After washing several times with PBS to remove NCI H929 cells, BMSCs were ready for AFM analysis.

2.7. Statistical analysis

Statistical analysis was carried out using a Student's *t*-test to discern differences of the data when appropriate. p values less than 0.05 were considered statistically significant.

3. Results

3.1. Myeloma cells modulate biomechanical properties of M-BMSCs

AFM is a reliable way to measure stiffness of living cells. One of its unique advantages is that it records micro-scale stiffness on individual cells, layers of cells or even on pieces of tissue [32]. A brief description of the AFM procedures is summarized in Fig. 1. Cells were indented 1000 nm with a spherical AFM probe. Cell stiffness (Young's modulus) was determined by fitting a Hertz model of a hard sphere indenting a soft, elastic surface to the data [30]. 30–60 single cells were detected for each condition. As shown in Fig. 1C, the mean stiffness of N-BMSCs, MGUS-BMSCs and M-BMSCs was 670 ± 20 Pa, 1360 ± 100 Pa and 1550 ± 100 Pa, respectively. The values quoted here were mean Young's moduli +/− SEM. Our data indicated that MGUS and M-BMSCs are stiffer than N-BMSCs. No significant difference was observed between M-BMSCs and MGUS-BMSCs. Since myeloma cells always attached to BMSCs, we tested the stiffness of BMSCs after co-culturing them with NIH 9292 myeloma cells for 24 h. There was no change in the stiffness of N-BMSCs (770 ± 40 Pa). The stiffness of M-BMSCs was significantly increased (2140 ± 180 Pa). There was a slight decrease in the stiffness of MGUS-BMSCs (960 ± 110 Pa); however this was not statistically significant (Fig. 1D). Our results indicated that myeloma cells were able to modify the biomechanical properties of M-BMSCs.

3.2. CD138$^-$ myeloma cells, but not CD138$^+$ cells, regulated M-BMSC stiffness

The cancer stem cell hypothesis postulates that only a small subpopulation of cells can initiate a tumor or cause a tumor relapse [33]. CD138$^-$ myeloma cells have been considered as myeloma initiating cells [15,34]. Since we found the myeloma cells induced biomechanical changes in M-BMSCs, the effect of CD138$^-$ myeloma cells on the biomechanical architecture of M-BMSCs is unknown. To test the effect of myeloma initiating cells on M-BMSC stiffness, we separated NCI H929 MM cells into CD138$^-$ and CD138$^+$ subpopulations. The stiffness of M-BMSCs was detected after coculturing with CD138$^+$ or CD138$^-$ cells. A significant increase in the stiffness (57.6%) of M-BMSCs was noted when co-cultured with CD138$^-$ cells compared with that determined in the non-cocultured M-BMSCs. No change in the stiffness of M-BMSCs was observed after co-culturing with CD138$^+$ cells (1290 ± 9 Pa) as shown in Fig. 2A. Our data suggested that CD138$^-$ cells played a key role in myeloma cells-mediated biomechanical changes of M-BMSCs.

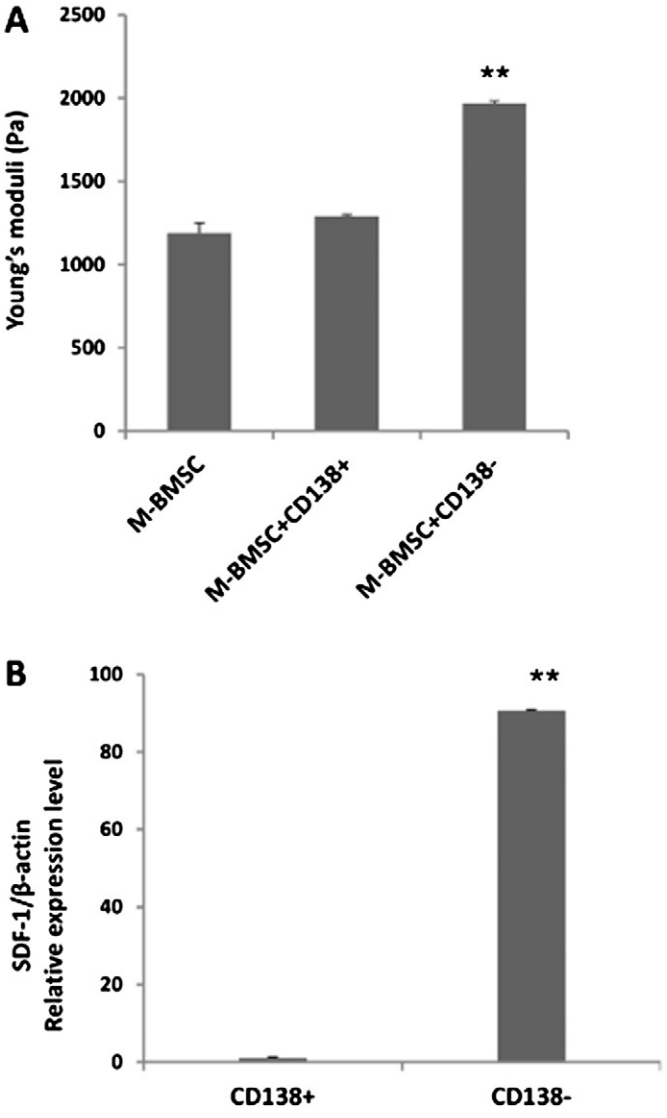

Fig. 2. CD138$^-$ myeloma cells, but not CD138$^+$ cells, regulated the stiffness of M-BMSCs. (A) CD138$^-$ and CD138$^+$ subpopulation of NCI H929 cells was isolated using MACS beads and co-cultured with M-BMSCs for 24 h, respectively. The stiffness of M-BMSCs was detected using AFM after removing CD138$^-$ or CD138$^+$ subpopulation of NCI H929 myeloma cells. Data was calculated from 33 cells of CD138$^+$ cells primed M-BMSCs, 30 CD138$^-$ cells primed M-BMSCs. (B) Total RNA was isolated from CD138$^-$ and CD138$^+$ cells and mRNA level of SDF-1 determined using qPCR. β-Actin was used as a loading control. All experiments were repeated 3 times. Mean ± SE, $^{**}p < 0.01$.

3.3. SDF-1/CXCR4 signaling was essential for the CD138$^-$ myeloma cells-enhanced stiffness of M-BMSCs

Earlier studies have shown that SDF-1 and its receptor CXCR4 are critical regulators of the interaction between MM cells and BMSCs [35]. To investigate if SDF-1/CXCR4 regulated the interaction between CD138$^-$ cells and BMSCs, we first compared the expression of SDF-1 in CD138$^+$ and CD138$^-$ myeloma subpopulations. SDF-1 mRNA levels were determined using qPCR. As shown in Fig. 2B, SDF-1 was highly expressed in CD138$^-$ myeloma cells compared to that in the CD138$^+$ cell subpopulation. To determine the direct effect of SDF-1 on BMSC stiffness, N-BMSCs, MGUS-BMSCs and M-BMSCs were treated with 100 ng/ml recombined SDF-1 for 2 h and then their moduli were measured using AFM. Treating M-BMSCs with SDF-1 led to a ~50% increase (from 1550 ± 70 Pa to 2050 ± 90 Pa) in the stiffness of cells. In contrast, the stiffness of N-BMSCs and MGUS-BMSCs remained unchanged (Fig. 3A). AMD3100 is a specific CXCR4 antagonist. Western blot

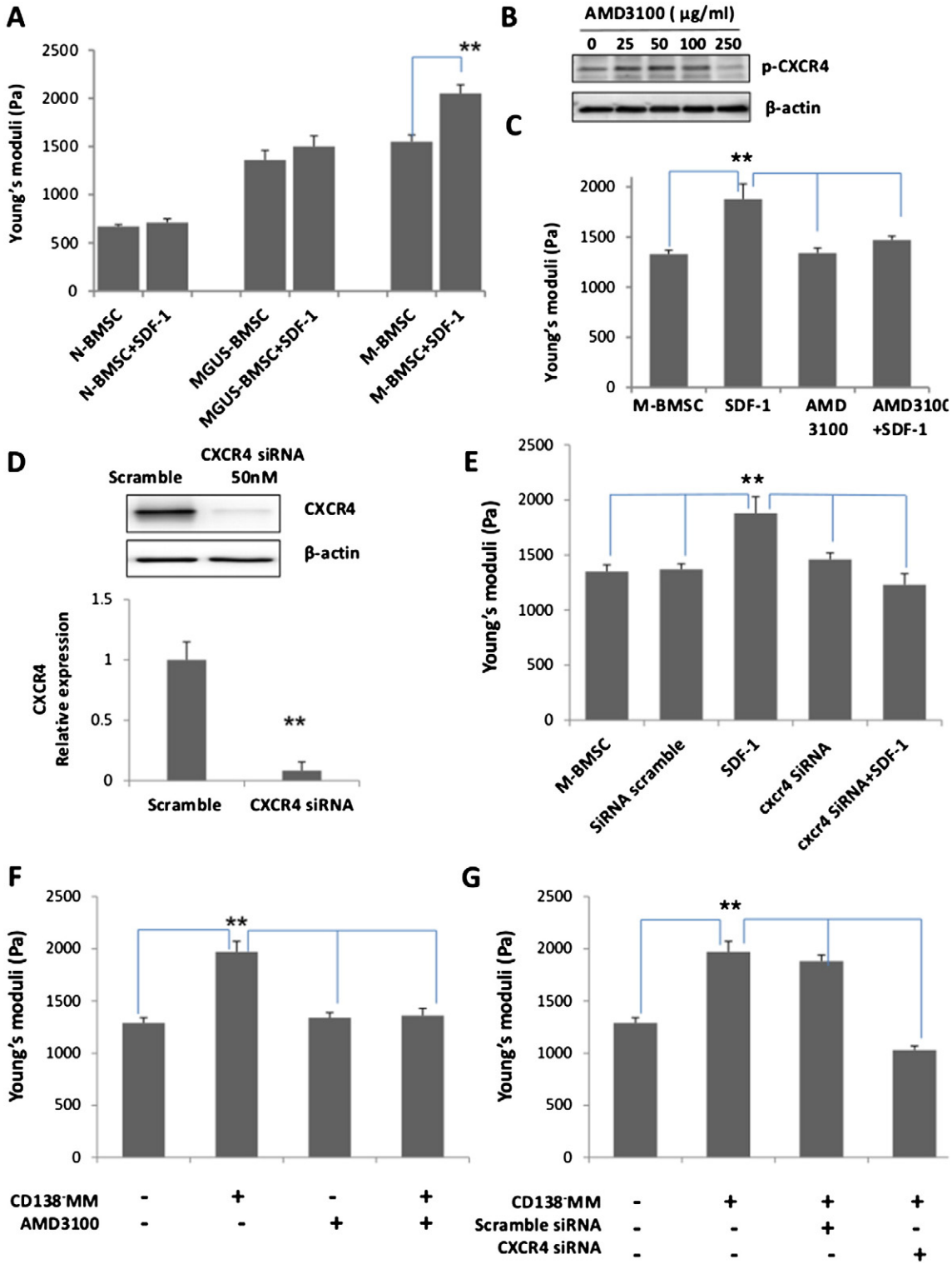

Fig. 3. CD138$^-$ myeloma cell-enhanced stiffness of M-BMSCs was regulated by SDF/CXCR4 signaling. A: Stiffness in M-BMSCs, MGUS-BMSCs and N-BMSCs after incubation for 2 h w/wo 100 ng/ml SDF-1. Data was calculated from 35 cells of M-BMSCs, 43 MGUS-BMSCs and 61 N-BMSCs. B: Representative Western blots showing the protein level of *p*-CXCR4 in AMD3100-treated and untreated M-BMSCs. C: Stiffness in M-BMSCs treated with 250 μg/ml AMD3100 and/or 100 ng/ml of SDF-1. Data was calculated from 35 cells of M-BMSCs, 30 SDF-1 treated M-BMSCs, 35 AMD3100 treated M-BMSCs, and 30 AMD3100 and SDF-1 treated M-BMSCs. D: Western blots and qPCR showing the protein level (upper panel) and gene expression (lower panel) of CXCR4 in M-BMSCs transiently transfected with CXCR4 or non-targeted scrambled RNAi. E: Stiffness in M-BMSCs that were transiently transfected with CXCR4 or scrambled RNAi and then treated with SDF-1. Data was calculated from 35 cells of M-BMSCs, 30 SDF-1 treated M-BMSCs, 30 siRNA scramble treated M-BMSCs, 30 CXCR4 siRNA treated M-BMSCs and 30 CXCR4 siRNA-SDF-1 treated M-BMSCs. F: Stiffness in M-BMSCs that preincubated AMD3100 and then cocultured with CD138$^-$ myeloma cells. Data was calculated from 35 cells of M-BMSCs, 30 CD138$^-$ cells primed M-BMSCs, 30 AMD3100 treated M-BMSCs, and 30 AMD3100-CD138$^-$ cells treated M-BMSCs. G: Stiffness in M-BMSCs that cocultured with CD138$^-$ cells and CD138$^-$ cells transfected with CXCR4 or scrambled RNAi. Data was calculated from 35 cells of M-BMSCs, 30 CD138$^-$ cells primed M-BMSCs, 30 siRNA scramble-CD138$^-$ cells primed M-BMSCs, and 30 CXCR4 siRNA-CD138$^-$ cells treated M-BMSCs. All experiments were repeated 3 times. Mean ± SE; **$p < 0.01$.

analysis showed that treating M-BMSCs with 250 μg/ml of AMD3100 inhibited CXCR4 phosphorylation (Fig. 3B). To determine if inhibition of CXCR4 affected SDF-1-elevated stiffness of M-BMSCs, M-BMSCs were incubated with AMD 3100 for 22 h and then treated with 100 ng/ml of SDF-1 for 2 h. Pretreatment with AMD3100 blocked the SDF-1-induced increase in the stiffness of M-BMSCs (Fig. 3C). To further confirm the role of SDF-1/CXCR-4 in BMSC stiffness, we knocked down CXCR4 expression in M-BMSCs using siRNA. Transient transfection of CXCR4 siRNA led to a >75% reduction in CXCR4 mRNA level (Fig. 3D). AFM analysis showed that knocking-down CXCR4 abolished SDF-1-induced increase in the stiffness of M-BMSCs (Fig. 3E). To determine the role of SDF1/CXCR4 signaling in CD138$^-$ myeloma cell-mediated stiffness of M-BMSCs, M-BMSCs were treated with AMD3100 or transfected with CXCR4 siRNA. Inhibition of SDF-1 by AMD3100 or CXCR4 siRNA blocked CD138$^-$ myeloma-induced increase in M-BMSC stiffness (Fig. 3F & G), suggesting that CD138$^-$ myeloma cells-enhanced stiffness of M-BMSCs was mediated through SDF-1/CXCR4 signaling.

3.4. Molecular alteration of stiffness-associated proteins in BMSCs following treatment with recombinant SDF-1 protein

To determine if treatment of BMSCs with SDF-1 modulated stiffness-associated proteins, M-BMSCs, MGUS-BMSCs and N-BMSCs were treated with recombinant SDF-1 and cell lysates harvested at 15 and 60 min post-treatment for protein analysis using Western blots. Focal adhesion kinase (FAK), RhoA and myosin light chain 2 (MLC) are proteins associated with cytoskeletal mechanics and cell contraction, which play an

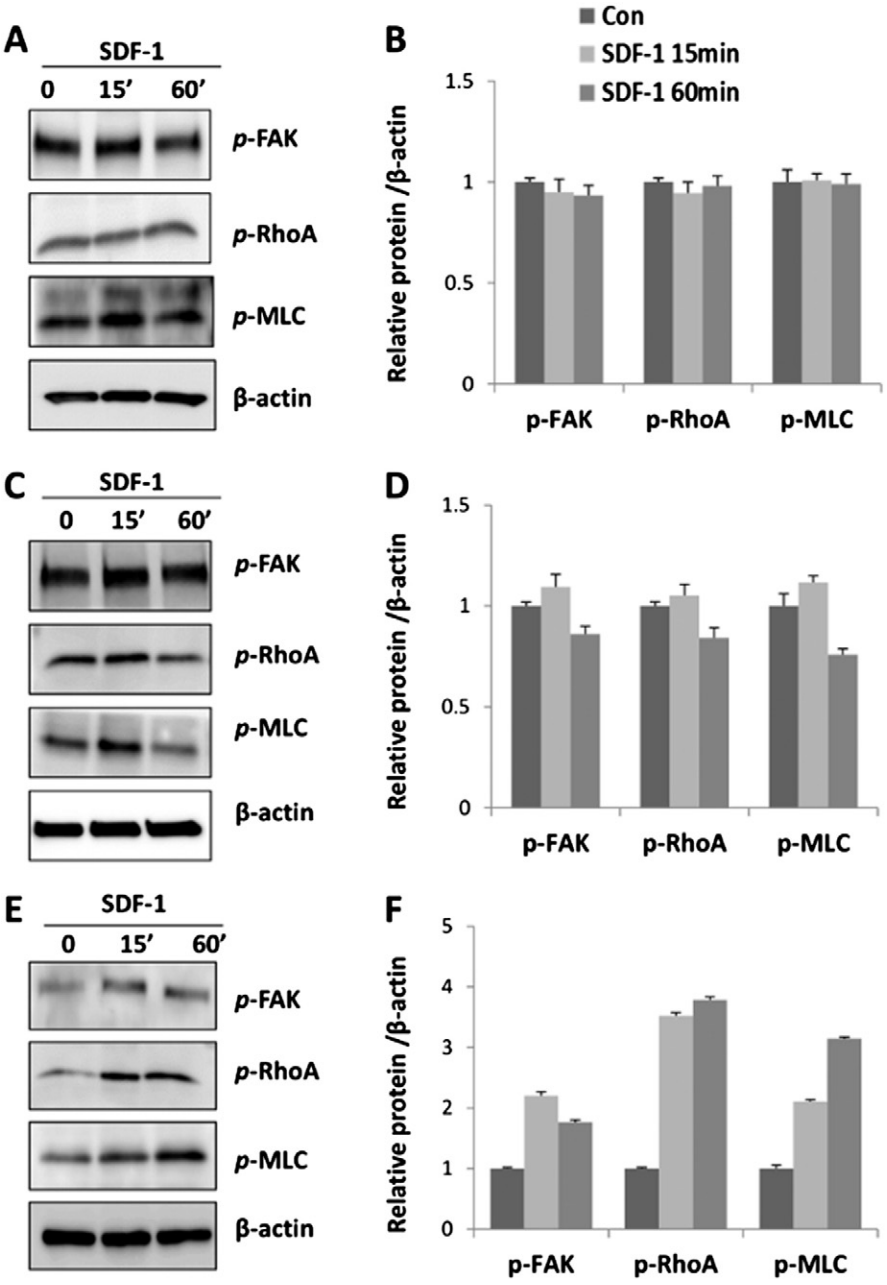

Fig. 4. The phosphorylation of FAK, RhoA and MLC proteins was differentially regulated by SDF-1 in M-, MGUS-, and N-BMSCs. A: Representative Western blots showing the protein levels of *p*-FAK, *p*-RhoA and *p*-MLC in N-BMSCs at 15 and 60 min post-treatment treatment with 100 ng/ml SDF-1. B: Densitometric quantification of the data showing in A. C. Representative Western blots showing the protein levels of *p*-FAK, p-RhoA and *p*-MLC in MGUS-BMSCs treated with SDF-1. D: Densitometric quantification of the data showing in C. E. Representative Western blots showing the protein levels of *p*-FAK, *p*-RhoA and *p*-MLC in M-BMSCs treated with SDF-1. F: Densitometric quantification of the data showing in E. All experiments have been repeated 3 times. Mean ± SE; $^{**}p < 0.01$.

important role in regulating cell stiffness [36–39]. Our data showed that the phosphorylated protein levels of FAK, RhoA, and MLC were unchanged (Fig. 4A, B, C & D) in N-BMSCs and MGUS-BMSCs, but significantly upregulated in M-BMSCs following treatment with SDF-1 (Fig. 4E & F).

3.5. AKT and FAK activation were required for SDF-1-mediated mechanical alteration of M-BMSCs

AKT activation has been linked with SDF-1/CXCR4-mediated tumor cell migration and angiogenesis [40]. We observed a marked increase in *p*-AKT protein level in M-BMSCs treated with SDF-1 (Fig. 5). Treating M-BMSCs using PI3K/AKT inhibitor LY294002 reduced *p*-AKT protein level (Fig. 6A). To determine the role of AKT activation in SDF-1-regulated cell stiffness, M-BMSCs were incubated with 50 μM LY294002 for 12 h and then treated with recombinant SDF-1 for 2 h. As shown in Fig. 6B, inhibition of AKT activation eliminated the SDF-1-induced increase in the stiffness of M-BMSCs.

Furthermore, we also detected the role of FAK activation in SDF-1-mediated M-BMSC stiffness. Cells were pre-incubated with 1 μM FAK inhibitor 14 for 12 h and then treated with SDF-1 for 2 h. As shown in Fig. 6C and D, inhibition of FAK activation abolished the SDF-1-induced increase in the stiffness of M-BMSCs.

4. Discussion

In the current study, we found that BMSCs collected from MM and MGUS patients were stiffer than those collected from healthy individuals. BMSCs from MM patients showed increased stiffness when cocultured with NCI-H929 MM cells, which was not observed in N-BMSCs and MGUS-BMSCs. $CD138^-$ myeloma cells, but not $CD138^+$ cells, expressed high level of SDF-1 and regulated M-BMSC stiffness. Inhibition of SDF-1 using a pharmacological inhibitor

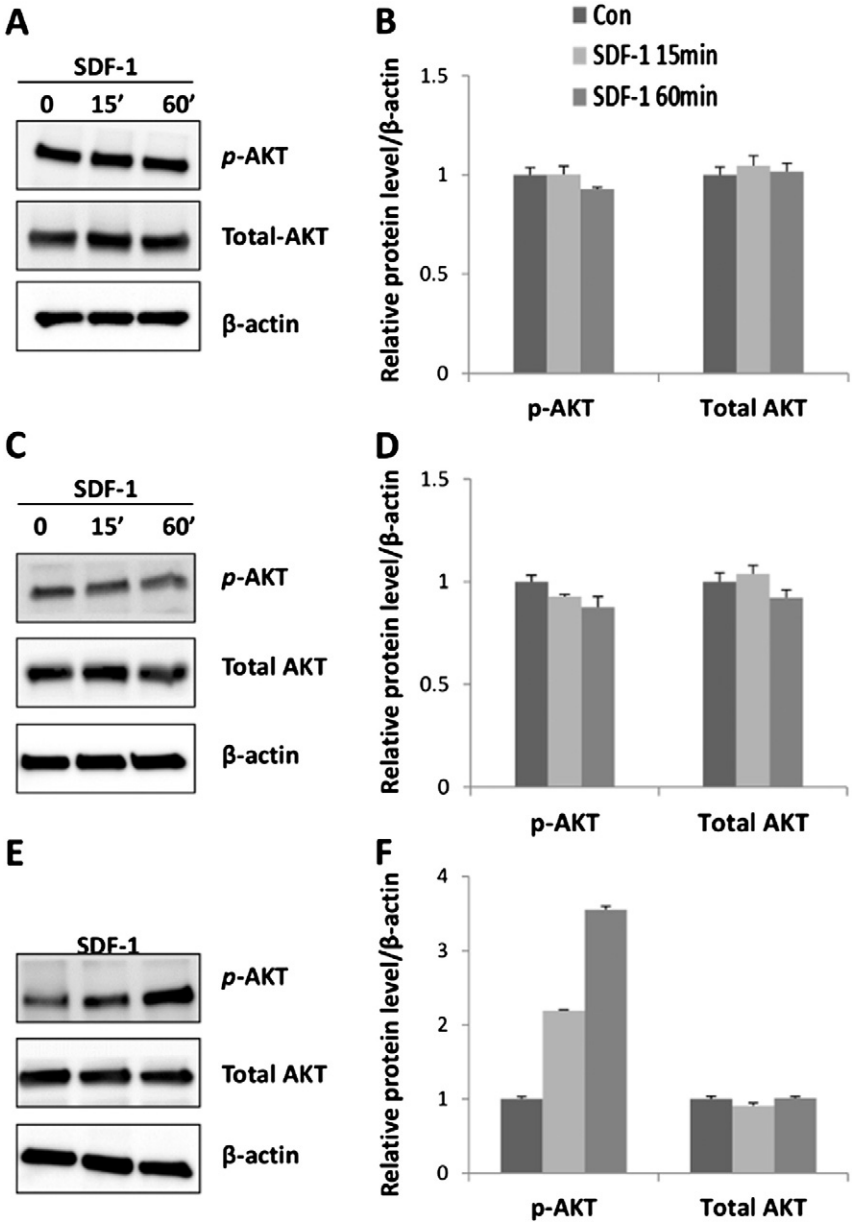

Fig. 5. Incubation with SDF-1 led to elevated phosphorylation of AKT in M-BMSCs. A: Representative Western blots showing the protein levels of *p*-AKT in N-BMSCs at 15 and 60 min post-treatment with 100 ng/ml SDF-1. B: Densitometric quantification of the data showing in A. C. Representative Western blots showing the protein level of *p*-AKT treated with SDF-1 in MGUS-BMSC. B: Densitometric quantification of the data showing in C. E. Representative Western blots showing the protein level of *p*-AKT in M-BMSCs treated with SDF-1. F: Densitometric quantification of the data showing in E. All experiments have been repeated 3 times, Mean ± SE; ** $p < 0.01$.

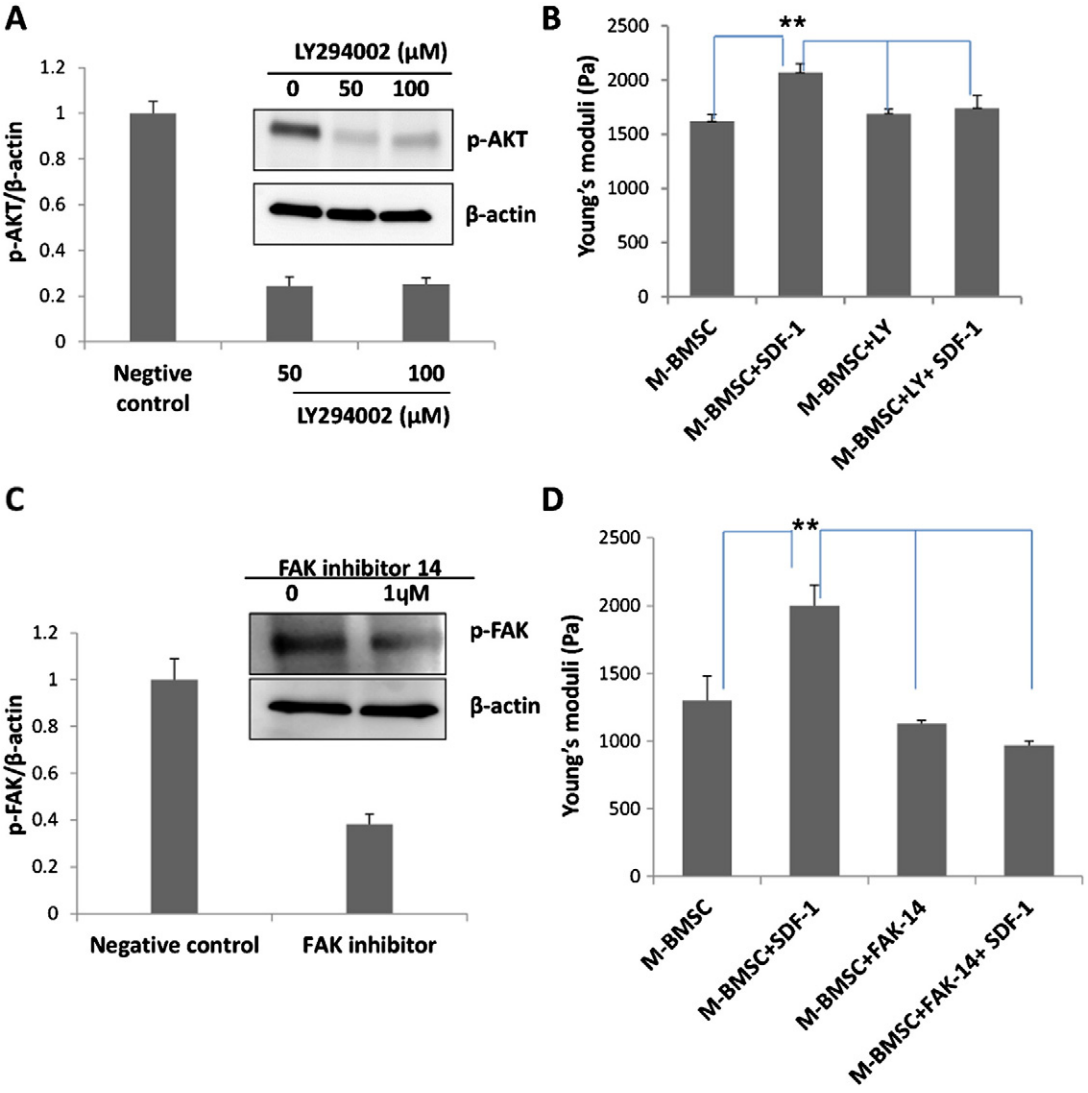

Fig. 6. Inhibition of AKT and FAK activation abolished SDF-1-enhanced increase in M-BMSC stiffness. A: M-BMSCs were incubated with 50 or 100 μM of LY294002 for 12 h and p-AKT protein level was determined by Western blot. Densitometric quantification of Western blot results indicated a reduction of *p*-AKT in LY294002-treated cells. B: M-BMSCs were incubated with 50 μM of LY294002 for 12 h and then treated with recombinant SDF-1 for 2 h. The stiffness of M-BMSCs was determined. Pre-incubation of M-BMSCs with LY294002 blocked SDF-1-induced increase of stiffness in M-BMSCs. Data was calculated from 35 cells of M-BMSCs, 30 SDF-1 treated M-BMSCs, 30 LY294002 treated M-BMSCs, and 30 LY294002-SDF-1 treated M-BMSCs. C: M-BMSCs were incubated with 1 μM of FAK inhibitor for 12 h and *p*-FAK protein level was determined by Western blot. Densitometric quantification of Western blot results indicated a reduction of *p*-FAK in FAK inhibitor-treated cells. D: M-BMSCs were incubated with 1 μM of FAK inhibitor for 12 h and then treated with recombinant SDF-1 for 2 h. The stiffness of M-BMSCs was determined. Pre-incubation of M-BMSCs with FAK inhibitor 14 blocked SDF-1-induced increase of stiffness in M-BMSCs. Data was calculated from 30 cells of M-BMSCs, 30 SDF-1 treated M-BMSCs, 30 FAK inhibitor treated M-BMSCs, and 30 FAK inhibitor-SDF-1 treated M-BMSCs. All experiments have been repeated 3 times, Mean ± SE, $^{**}p < 0.01$.

or knocking-down CXCR4 in M-BMSCs abolished $CD138^-$ myeloma cells-induced increase in M-BMSC stiffness, suggesting an important role of SDF-1/CXCR4 signaling.

Interactions of tumor cells with their surrounding microenvironment have been known to impact tumor initiation, progression and metastasis, as well as patient prognosis [41]. The mechanical properties of stroma can govern cellular behavior of tumors through a variety of biochemical and biophysical mechanisms. Using an in vitro system of matrix-coated polyacrylamide gels, Schrader et al. found that increasing matrix stiffness promoted hepatocellular carcinoma cell proliferation [42]. Weaver and Kumar reported that cross-linked ECM collagen increased ECM stiffness and promoted malignancy [43]. Paszek et al. found that matrix stiffness promoted malignant transformation of a tissue [24]. Preclinical studies using mouse models showed that cancer cells were more proliferative and migrative on the stiff microenvironment [44]. Adhesion of MM to BMSCs has been suggested to be crucial for myeloma cell proliferation and drug resistance. BMSC production of matrix proteins and factors such as fibronectin [6], insulin-like growth factor-1 (IGF-1) [7], stromal derived factor 1 alpha (SDF-1) [8], tumor necrosis factor alpha (TNF-α), B cell activating factor family (BAFF), and a proliferation inducing ligand (APRIL) [5] has all been shown to promote MM cell proliferation and resistance to conventional chemotherapeutic agents. Corre et al. reported that BMSCs from MM patients had a distinctive gene expression profile comparing with normal BMSCs [45]. A total of 79 genes in BMSCs from MM patients were overexpressed and 46% of them involved in tumor-microenvironment cross-talk. It has been reported that myeloma BMSCs increase the colony-forming ability, growth and survival of myeloma stem cells as compared with normal BMSCs [26]. Fuhler and his colleagues have proved that increased numbers of $CD138^-$ cells and cell–cell adhesion observed upon myeloma cells cultured with BMSC [46]. BMSC revert myeloma cells to less differentiated phenotype by combined activities of adhesive interactions and IL6, which might contribute to stromal cell-conferred drug resistance [47]. The interaction between the

components of tumor environment and tumor cells is bidirectional. Tumor cells can also attract or activate tumor-associated stromal cells by releasing a number of growth factor, cytokines and chemokines to facilitate their growth, invasion and metastasis [48–50]. An early study reported that BMSCs from MM patients were significantly stiffer than BMSCs obtained from healthy volunteers using a cytocompression device [25]. Our results indicated that higher stiffness of BMSCs was not a unique feature of M-BMSCs. MGUS-BMSCs were also stiffer than N-BMSCs. The stiffness of M-BMSCs was further enhanced when cocultured with myeloma cells.

Though the cancer stem cell is still a debatable concept, $CD138^-$ myeloma subpopulation has been recognized as MM initiating cells in several studies [15,34]. Why myeloma is incurable and relapses in multiple myeloma patients is still unknown. One potential mechanism is that myeloma initiating cells or stem cells are capable of escaping from the effects of chemotherapy/radiotherapy and growing into mature myeloma cells. Identifying the communication between myeloma initiating cells and the bone marrow microenvironment might facilitate the development of new strategies to halt progression of the disease. We found that $CD138^-$ myeloma cell-primed M-BMSCs became stiffer than non-primed counterparts. No change in the stiffness of M-BMSCs was observed after co-culturing with $CD138^+$ cells. These results suggest that $CD138^-$ myeloma cells play an important role in regulating biomechanical properties of M-BMSCs. Our studies demonstrated the cross-talk between myeloma initiating cells with BMSCs.

Gene expression profiling analysis shows that mRNA level of SDF-1 is low in both primary myeloma cells and M-BMSCs comparing with that from their healthy counterparts [45,51]. Interestingly, when we analyzed mRNA level of SDF-1 in $CD138^+$ and $CD138^-$ MM cells using qPCR, we found that SDF-1 was highly expressed in $CD138^-$ cells when compared with that in the $CD138^+$ subpopulation (Fig. 2D). SDF-1 is secreted by bone marrow endothelial cells, BMSC, immature osteoblasts, primary malignant plasma cells and myeloma cells [52,53] and it is a critical regulator of myeloma cell migration, homing and adhesion to stromal cell [35,54]. Our results showed that SDF-1 regulates the stiffness of M-BMSCs, but not N-BMSCs or MGUS-BMSCs. Inhibition of SDF1 signaling, using either a pharmaceutical inhibitor or knocking-down SDF-1 receptor CXCR4 in M-BMSCs, abolished the $CD138^-$ myeloma cell-induced increase in the stiffness of M-BMSCs. This suggests that the SDF-1/CXCR4 signaling pathway is responsible for $CD138^-$ myeloma cell-mediated mechanical changes in M-BMSCs.

FAK plays an important role in cell adhesion and regulation of cellular mechanical properties. FAK has been reported to increase cell stiffness and contractile force [55]. Rho GTPases are key regulators of cytoskeletal tension that are correlated with increased stress fiber formation, cell stiffness, integrin activation and myosin phosphorylation [56]. MLC has been shown to promote cell contractility. Cell stiffness is strongly regulated by phosphorylation of MLC subunit on the Ser19 [57,58]. Therefore, we used FAK, RhoA and MLC as molecular markers of cell stiffness. Western blotting analysis showed that the phosphorylated protein levels of FAK, RhoA and MLC were increased in SDF-1 treated M-BMSCs.

The SDF-1/CXCR4 axis has been reported to regulate tumor cell proliferation and migration through activation of several signaling pathways [40,52], including PI3K/AKT. AKT and FAK were specifically activated in the M-BMSCs following treatment with SDF-1, which was not seen in other BMSCs. AKT and FAK are two important kinases to regulated tumor cell adhesion, invasion and migration [59,60]. Blockage of AKT and FAK activity using selective inhibitors abolished SDF-1-induced mechanical changes in M-BMSCs. Our data indicated that both AKT and FAK activation are required for the action of SDF-1 in M-BMSCs.

5. Conclusions

Our studies demonstrate that (1) M-BMSCs and MGUS-BMSCs had increased stiffness compared with N-BMSCs; (2) MM cells enhanced the stiffness of M-BMSCs; (3) $CD138^-$ myeloma cells, but not $CD138^+$ cells, upregulated the stiffness of M-BMSCs; (4) $CD138^-$ myeloma cell-induced increase in M-BMSC stiffness was mediated by SDF-1/CXCR4 signaling pathways; and (5) AKT and FAK activation was required for SDF-1-enhanced M-BMSC stiffness. To the best of our knowledge, this is the first study to demonstrate myeloma cell-directed tumor-BMSC communication and delineate the role of $CD138^-$ myeloma cells and SDF-1 in regulation of M-BMSC stiffness. Further understanding of the mechanism (s)-associated with myeloma initiating cells with their various components of their microenvironment can help us identify new therapeutic targets for treatment of MM.

Financial support

NIH grant U01CA166886 (X.Z.), National Science Foundation Materials and Surface Engineering grant CMMI-1152781 (K.B. and M.G.) and a pilot grant from the Center for Molecular Communication and Signaling at Wake Forest University (U01057).

Acknowledgments

This work was supported by NIH grant U01CA166886 (X.Z.), and a pilot grant from the Center for Molecular Communication and Signaling at Wake Forest University (U01057). This material is based upon the work supported by the National Science Foundation under Grant Number 1106105 (K.B. and M.G.). The authors would like to thank Dr. Glen Marrs, director of the WFU Microscopic Imaging Core Facility, for his assistance in SEM images.

References

[1] A. Falanga, M. Marchetti, Venous thromboembolism in the hematologic malignancies, J. Clin. Oncol. 27 (29) (2009) 4848–4857.
[2] Health., U.S.N.I.o, SEER (Surveillance, Epidemiology, and End Results Program) Stat Fact Sheet: MyelomaAvailable at http://seer.cancer.gov/statfacts/html/mulmy.html (Accessed March 15, 2014).
[3] R.A. Kyle, T.M. Therneau, S.V. Rajkumar, J.R. Offord, D.R. Larson, M.F. Plevak, et al., A long-term study of prognosis in monoclonal gammopathy of undetermined significance, N. Engl. J. Med. 346 (8) (2002) 564–569.
[4] R.A. Kyle, S.V. Rajkumar, Monoclonal gammopathy of undetermined significance, Br. J. Haematol. 134 (6) (2006) 573–589.
[5] R.A. Kyle, T.M. Therneau, S.V. Rajkumar, D.R. Larson, M.F. Plevak, J.R. Offord, et al., Prevalence of monoclonal gammopathy of undetermined significance, N. Engl. J. Med. 354 (13) (2006) 1362–1369.
[6] T. Hideshima, C. Mitsiades, G. Tonon, P.G. Richardson, K.C. Anderson, Understanding multiple myeloma pathogenesis in the bone marrow to identify new therapeutic targets, Nat. Rev. Cancer 7 (8) (2007) 585–598.
[7] D. Pulte, M.T. Redaniel, H. Brenner, L. Jansen, M. Jeffreys, Recent improvement in survival of patients with multiple myeloma: variation by ethnicity, Leuk. Lymphoma 55 (5) (2014) 1083–1089.
[8] S. Manier, A. Sacco, X. Leleu, I.M. Ghobrial, A.M. Roccaro, Bone marrow microenvironment in multiple myeloma progression, J. Biomed. Biotechnol. 2012 (2012) 157496.
[9] T. Hideshima, P.L. Bergsagel, W.M. Kuehl, K.C. Anderson, Advances in biology of multiple myeloma: clinical applications, Blood 104 (3) (2004) 607–618.
[10] Y. Nefedova, P. Cheng, M. Alsina, W.S. Dalton, D.I. Gabrilovich, Involvement of Notch-1 signaling in bone marrow stroma-mediated de novo drug resistance of myeloma and other malignant lymphoid cell lines, Blood 103 (9) (2004) 3503–3510.
[11] S. Kumar, T.E. Witzig, M. Timm, J. Haug, L. Wellik, R. Fonseca, et al., Expression of VEGF and its receptors by myeloma cells, Leukemia 17 (10) (2003) 2025–2031.
[12] G. Schwab, C.B. Siegall, L.A. Aarden, L.M. Neckers, R.P. Nordan, Characterization of an interleukin-6-mediated autocrine growth loop in the human multiple myeloma cell line, U266, Blood 77 (3) (1991) 587–593.
[13] M.A. Frassanito, A. Cusmai, G. Iodice, F. Dammacco, Autocrine interleukin-6 production and highly malignant multiple myeloma: relation with resistance to drug-induced apoptosis, Blood 97 (2) (2001) 483–489.
[14] W.C. Cheung, B. Van Ness, The bone marrow stromal microenvironment influences myeloma therapeutic response in vitro, Leukemia 15 (2) (2001) 264–271.
[15] W. Matsui, Q. Wang, J.P. Barber, S. Brennan, B.D. Smith, I. Borrello, et al., Clonogenic multiple myeloma progenitors, stem cell properties, and drug resistance, Cancer Res. 68 (1) (2008) 190–197.
[16] W. Matsui, C.A. Huff, Q. Wang, M.T. Malehorn, J. Barber, Y. Tanhehco, et al., Characterization of clonogenic multiple myeloma cells, Blood 103 (6) (2004) 2332–2336.
[17] K. Tarte, J. De Vos, T. Thykjaer, F. Zhan, G. Fiol, V. Costes, et al., Generation of polyclonal plasmablasts from peripheral blood B cells: a normal counterpart of malignant plasmablasts, Blood 100 (4) (2002) 1113–1122.

[18] R. Reghunathan, C. Bi, S.C. Liu, K.T. Loong, T.H. Chung, G. Huang, et al., Clonogenic multiple myeloma cells have shared stemness signature assocuated with patient survival, Oncotarget 4 (8) (2013) 1230–1240.
[19] N. Hosen, Y. Matsuoka, S. Kishida, J. Nakata, Y. Mizutani, K. Hasegawa, et al., CD138-negative clonogenic cells are plasma cells but not B cells in some multiple myeloma patients, Leukemia 26 (9) (2012) 2135–2141.
[20] W. Zhou, Y. Yang, Z. Gu, H. Wang, J. Xia, X. Wu, et al., ALDH1 activity identifies tumor-initiating cells and links to chromosomal instability signatures in multiple myeloma, Leukemia 28 (2014) 1155–1158.
[21] A. Chaidos, C.P. Barnes, G. Cowan, P.C. May, V. Melo, E. Hatjiharissi, et al., Clinical drug resistance linked to interconvertible phenotypic and functional states of tumor-propagating cells in multiple myeloma, Blood 121 (2) (2013) 318–328.
[22] R.W. Tilghman, C.R. Cowan, J.D. Mih, Y. Koryakina, D. Gioeli, J.K. Slack-Davis, et al., Matrix rigidity regulates cancer cell growth and cellular phenotype, PLoS One 5 (9) (2010) e12905.
[23] T.A. Ulrich, E.M. de Juan Pardo, S. Kumar, The mechanical rigidity of the extracellular matrix regulates the structure, motility, and proliferation of glioma cells, Cancer Res. 69 (10) (2009) 4167–4174.
[24] M.J. Paszek, N. Zahir, K.R. Johnson, J.N. Lakins, G.I. Rozenberg, A. Gefen, et al., Tensional homeostasis and the malignant phenotype, Cancer Cell 8 (3) (2005) 241–254.
[25] Y. Feng, G. Ofek, D.S. Choi, J. Wen, J. Hu, H. Zhao, et al., Unique biomechanical interactions between myeloma cells and bone marrow stroma cells, Prog. Biophys. Mol. Biol. 103 (1) (2010) 148–156.
[26] Y. Feng, J. Wen, P. Mike, D.S. Choi, C. Eshoa, Z.Z. Shi, et al., Bone marrow stromal cells from myeloma patients support the growth of myeloma stem cells, Stem Cells Dev. 19 (9) (2010) 1289–1296.
[27] C.R. Carlisle, C. Coulais, M. Namboothiry, D.L. Carroll, R.R. Hantgan, M. Guthold, The mechanical properties of individual, electrospun fibrinogen fibers, Biomaterials 30 (6) (2009) 1205–1213.
[28] W. Liu, L.M. Jawerth, E.A. Sparks, M.R. Falvo, R.R. Hantgan, R. Superfine, et al., Fibrin fibers have extraordinary extensibility and elasticity, Science 313 (5787) (2006) 634.
[29] L. Peng, B.J. Stephens, K. Bonin, R. Cubicciotti, M. Guthold, A combined atomic force/fluorescence microscopy technique to select aptamers in a single cycle from a small pool of random oligonucleotides, Microsc. Res. Tech. 70 (4) (2007) 372–381.
[30] C.D. Markert, X. Guo, A. Skardal, Z. Wang, S. Bharadwaj, Y. Zhang, et al., Characterizing the micro-scale elastic modulus of hydrogels for use in regenerative medicine, J. Mech. Behav. Biomed. Mater. 27 (2013) 115–127.
[31] R. Vargas-Pinto, H. Gong, A. Vahabikashi, M. Johnson, The effect of the endothelial cell cortex on atomic force microscopy measurements, Biophys. J. 105 (2) (2013) 300–309.
[32] M. Plodinec, M. Loparic, C.A. Monnier, E.C. Obermann, R. Zanetti-Dallenbach, P. Oertle, et al., The nanomechanical signature of breast cancer, Nat. Nanotechnol. 7 (11) (2012) 757–765.
[33] S. Kleffel, T. Schatton, Tumor dormancy and cancer stem cells: two sides of the same coin? Adv. Exp. Med. Biol. 734 (2013) 145–179.
[34] Y. Yang, J. Shi, G. Tolomelli, H. Xu, J. Xia, H. Wang, et al., RARalpha2 expression confers myeloma stem cell features, Blood 122 (8) (2013) 1437–1447.
[35] A.K. Azab, F. Azab, S. Blotta, C.M. Pitsillides, B. Thompson, J.M. Runnels, et al., RhoA and Rac1 GTPases play major and differential roles in stromal cell-derived factor-1-induced cell adhesion and chemotaxis in multiple myeloma, Blood 114 (3) (2009) 619–629.
[36] N. Kakinuma, B.C. Roy, Y. Zhu, Y. Wang, R. Kiyama, Kank regulates RhoA-dependent formation of actin stress fibers and cell migration via 14-3-3 in PI3K-Akt signaling, J. Cell Biol. 181 (3) (2008) 537–549.
[37] B. Fabry, A.H. Klemm, S. Kienle, T.E. Schaffer, W.H. Goldmann, Focal adhesion kinase stabilizes the cytoskeleton, Biophys. J. 101 (9) (2011) 2131–2138.
[38] S. Cai, L. Pestic-Dragovich, M.E. O'Donnell, N. Wang, D. Ingber, E. Elson, et al., Regulation of cytoskeletal mechanics and cell growth by myosin light chain phosphorylation, Am. J. Physiol. 275 (5 Pt 1) (1998) C1349–C1356.
[39] K.M. Stroka, H. Aranda-Espinoza, Endothelial cell substrate stiffness influences neutrophil transmigration via myosin light chain kinase-dependent cell contraction, Blood 118 (6) (2011) 1632–1640.
[40] J. Wang, J. Wang, Y. Sun, W. Song, J.E. Nor, C.Y. Wang, et al., Diverse signaling pathways through the SDF-1/CXCR4 chemokine axis in prostate cancer cell lines leads to altered patterns of cytokine secretion and angiogenesis, Cell. Signal. 17 (12) (2005) 1578–1592.
[41] J.A. Joyce, J.W. Pollard, Microenvironmental regulation of metastasis, Nat. Rev. Cancer 9 (4) (2009) 239–252.
[42] J. Schrader, T.T. Gordon-Walker, R.L. Aucott, M. van Deemter, A. Quaas, S. Walsh, et al., Matrix stiffness modulates proliferation, chemotherapeutic response, and dormancy in hepatocellular carcinoma cells, Hepatology 53 (4) (2011) 1192–1205.
[43] S. Kumar, V.M. Weaver, Mechanics, malignancy, and metastasis: the force journey of a tumor cell, Cancer Metastasis Rev. 28 (1–2) (2009) 113–127.
[44] M.S. Samuel, J.I. Lopez, E.J. McGhee, D.R. Croft, D. Strachan, P. Timpson, et al., Actomyosin-mediated cellular tension drives increased tissue stiffness and beta-catenin activation to induce epidermal hyperplasia and tumor growth, Cancer Cell 19 (6) (2011) 776–791.
[45] J. Corre, K. Mahtouk, M. Attal, M. Gadelorge, A. Huynh, S. Fleury-Cappellesso, et al., Bone marrow mesenchymal stem cells are abnormal in multiple myeloma, Leukemia 21 (5) (2007) 1079–1088.
[46] G.M. Fuhler, M. Baanstra, D. Chesik, R. Somasundaram, A. Seckinger, D. Hose, et al., Bone marrow stromal cell interaction reduces syndecan-1 expression and induces kinomic changes in myeloma cells, Exp. Cell Res. 316 (11) (2010) 1816–1828.
[47] N. Dezorella, M. Pevsner-Fischer, V. Deutsch, S. Kay, S. Baron, R. Stern, et al., Mesenchymal stromal cells revert multiple myeloma cells to less differentiated phenotype by the combined activities of adhesive interactions and interleukin-6, Exp. Cell Res. 315 (11) (2009) 1904–1913.
[48] I.P. Witz, Tumor-microenvironment interactions: dangerous liaisons, Adv. Cancer Res. 100 (2008) 203–229.
[49] H. Ungefroren, S. Sebens, D. Seidl, H. Lehnert, R. Hass, Interaction of tumor cells with the microenvironment, Cell Commun. Signal 9 (2011) 18.
[50] H. Lu, W. Ouyang, C. Huang, Inflammation, a key event in cancer development, Mol. Cancer Res. 4 (4) (2006) 221–233.
[51] F. Zhan, J. Hardin, B. Kordsmeier, K. Bumm, M. Zheng, E. Tian, et al., Global gene expression profiling of multiple myeloma, monoclonal gammopathy of undetermined significance, and normal bone marrow plasma cells, Blood 99 (5) (2002) 1745–1757.
[52] L. Mirandola, L. Apicella, M. Colombo, Y. Yu, D.G. Berta, N. Platonova, et al., Anti-Notch treatment prevents multiple myeloma cells localization to the bone marrow via the chemokine system CXCR4/SDF-1, Leukemia 27 (7) (2013) 1558–1566.
[53] S.Y. Kim, C.H. Lee, B.V. Midura, C. Yeung, A. Mendoza, S.H. Hong, et al., Inhibition of the CXCR4/CXCL12 chemokine pathway reduces the development of murine pulmonary metastases, Clin. Exp. Metastasis 25 (3) (2008) 201–211.
[54] Y. Alsayed, H. Ngo, J. Runnels, X. Leleu, U.K. Singha, C.M. Pitsillides, et al., Mechanisms of regulation of CXCR4/SDF-1 (CXCL12)-dependent migration and homing in multiple myeloma, Blood 109 (7) (2007) 2708–2717.
[55] C.T. Mierke, The role of focal adhesion kinase in the regulation of cellular mechanical properties, Phys. Biol. 10 (6) (2013) 065005.
[56] J.T. Parsons, A.R. Horwitz, M.A. Schwartz, Cell adhesion: integrating cytoskeletal dynamics and cellular tension, Nat. Rev. Mol. Cell Biol. 11 (9) (2010) 633–643.
[57] D.T. Butcher, T. Alliston, V.M. Weaver, A tense situation: forcing tumour progression, Nat. Rev. Cancer 9 (2) (2009) 108–122.
[58] V. Swaminathan, K. Mythreye, E.T. O'Brien, A. Berchuck, G.C. Blobe, R. Superfine, Mechanical stiffness grades metastatic potential in patient tumor cells and in cancer cell lines, Cancer Res. 71 (15) (2011) 5075–5080.
[59] S. Wang, M.D. Basson, Akt directly regulates focal adhesion kinase through association and serine phosphorylation: implication for pressure-induced colon cancer metastasis, Am. J. Physiol. Cell Physiol. 300 (3) (2011) C657–C670.
[60] N.G. Yousif, Fibronectin promotes migration and invasion of ovarian cancer cells through up-regulation of FAK-PI3K/Akt pathway, Cell Biol. Int. 38 (1) (2014) 85–91.